Diffuse Scattering Model of Indoor Wideband Propagation

Franek, Ondrej; Andersen, Jørgen Bach; Pedersen, Gert Frølund

Published in:
I E E E Transactions on Antennas and Propagation

DOI (link to publication from Publisher):
10.1109/TAP.2011.2158791

Publication date:
2011

Document Version
Accepted author manuscript, peer reviewed version

Diffuse Scattering Model of Indoor Wideband Propagation

Ondřej Franek, *Member, IEEE,* Jørgen Bach Andersen, *Life Fellow, IEEE,* and Gert Frølund Pedersen

***Abstract*—This paper presents a discrete-time numerical algorithm for computing field distributions in indoor environments by diffuse scattering from the walls. Calculations are performed for a rectangular room with semi-reflective walls. The walls are divided into 0.5 × 0.5 m segments, resulting in 2272 wall segments in total and approximately 2 min running time on average computer. Frequency independent power levels at the walls around the circumference of the room and at four receiver locations in the middle of the room are observed. It is demonstrated that after a finite period of initial excitation the field intensity in all locations eventually follows an exponential decay with the same slope and approximately the same level for given delay. These observations are shown to be in good agreement with theory and previous measurements—the slopes of the decay curves for measurement, simulation and theory are found to be 18 dB, 19.4 dB and 20.2 dB per 100 ns, respectively. The remaining differences are further discussed and an additional case of a spherical room is used to demonstrate the influence of the room shape on the results. It is concluded that the presented method is valid as a simple tool for use in indoor radio coverage predictions.**

***Index Terms*—Indoor radio communication, diffuse fields, numerical methods, propagation**

I. Introduction

In order to achieve a high degree of quality of service in wireless communication systems, the mobile device needs to maintain sufficient level of signal strength from the base station at all possible locations. This brings about a need for predicting the radio coverage from the base station, so that we can choose adequate radiated power and optimize the position of the base station antenna, or reduce their number if multiple access points are necessary in the given conditions. The character of the problem and its solution depends on the scale and complexity of the propagation environment, and two distinct scenarios, indoor and outdoor, are usually considered when choosing the appropriate method.

This work is focused on prediction of radiowave propagation in indoor environments, with application to personal communication systems in the centimeter-wave frequency range. Various methods have been employed to solve similar problems, the most prominent likely being ray tracing [1]. However, ray tracing accounts only for propagation by means of specular reflections or diffractions, but not diffuse scattering, which we see as more important, if not crucial, taking into consideration the commonly used wavelengths of wireless systems (cm) and comparable sizes of common room obstacles and surface structures. Drawbacks of the ray tracing approach with respect to diffuse scattering prediction are discussed in [2].

There have also been attempts to tackle the coverage problem with the finite-difference time-domain (FDTD) method, most recently in [3]. Nevertheless, the FDTD method is, in spite of steadily increasing computer speed and memory, still very demanding in terms of computational resources. As a result, FDTD studies are usually limited to two-dimensional algorithms and employ frequency reduction techniques in order to keep sufficient sampling per wavelength without memory exploding [3].

In a recent work [4], the concept of *room electromagnetics* was introduced, in analogy to room acoustics, a well-established discipline of predicting a sound field in a room. The idea is based on similarity of the wavelengths for both audio frequencies and microwave frequencies, whereas the size of the room and the roughness of the walls are expected to produce similar reverberation effects. Trying to obtain a numerical model to support the theory, we chose the *radiosity* method, which is based on purely diffuse scattering and has been successfully used in the acoustics discipline [5], as well as in computer graphics and architectural lighting [6]. The radiosity approach has also been employed in radio coverage prediction in outdoor studies [7]–[9] and in combination with ray tracing in indoor environment [10]. Among its advantages we would like to highlight the relative simplicity and speed of the algorithm, while the lack of any information on specular reflections might be seen as a disadvantage. It is also a power based method, in the sense that all phase and polarization information is missing. However, these are supposed to have random character anyway in most common scenarios of rooms with rough surfaces.

It should be noted that the observed similarity between the acoustic and electromagnetic waves is purely mathematical, not physical. Propagation effects are governed by the wave equation in both cases, and the relation of free space velocities and used frequencies results in comparable wavelengths and thus comparable propagation effects. Nevertheless, media different from air (e.g. walls, floors, water, ground) will, of course, have different propagation properties for either type of wave and cannot be interchanged.

Another difference is that electromagnetic waves are transverse and exhibit polarization effects, whereas acoustic waves are longitudinal. However, both polarizations are represented

Manuscript received July 20, 2010; revised January 5, 2011. This work was supported by the Danish Center for Scientific Computing.

O. Franek, J. B. Andersen and G. F. Pedersen are with the Antennas, Propagation and Radio Networking section, Department of Electronic Systems, Aalborg University, DK-9220 Aalborg Øst, Denmark (e-mail: franek@ieee.org, jba@es.aau.dk, gfp@es.aau.dk)

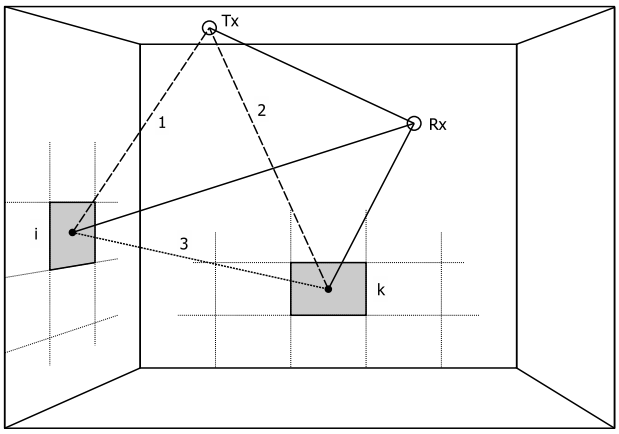

Fig. 1. Ray paths in a rectangular room (dashed: direct rays from transmitter to segments, dotted: scattering between segments, continuous: rays from transmitter and segments towards receiver).

equally in diffuse field and therefore can be treated together. In a real situation, the receiving antenna will usually pick up only one polarization of the incoming wave and the measured field may then be up to 3 dB lower than levels predicted by the radiosity model.

The goal of the present paper is to demonstrate that the radiosity method, despite some differences between its original domain and electromagnetics as described above, can be successfully applied to radiowave coverage prediction in indoor environments. The novelty of the work lies in application of the method to the important communication bands in the microwave and millimeter region. The results are compared with measurement around 6 GHz in realistic environment.

The paper is organized as follows. In Section II the diffuse scattering model is described and the formulas necessary for implementing the numerical algorithm are given. Section III then presents a simple numerical example together with impulse responses in discrete points in the room, angular responses and responses at the walls along the circumference of the room. Mean power quantities are shown, and measurement results from earlier paper are also included. Section IV proceeds with discussion of the results and their comparison to theoretical expectations from the field of acoustics. The work is concluded in Section V and some remarks about a successful implementation are drawn.

II. Problem Description

The walls of the room are divided into segments of area ΔS. We assume Lambertian diffuse scattering in lack of better information and the same scattering coefficient from each segment, although this is not a condition for the model. Lambertian scattering means that the scattering cross sections are proportional to cosine to the angle measured from the normal. This means that there is no scattering between segments along the same wall. The algorithm may be explained with reference to Fig. 1.

At time $t = 1\Delta t$, where Δt is the time step and number 1 represents the first discrete time instance, the transmitter (Tx) sends out an impulse. The shape of the impulse is not critical, as the radiosity algorithm does not support dispersion and all power contributions are simply added; the pulse width should only be short compared with the length of the time step. Next, the strengths of scattering sources are determined by simple free space radiation from Tx to segment i as ray 1 and ray 2 for segment k, denoted by dashed lines in Fig. 1. These are the incident fields and they are stored under the relevant delays 1 and 2, which are quantized so that all rays falling within the same time span Δt are added together in power. Segment k is also illuminated by segment i via ray 3 with the delay 1+3, and vice versa. The process keeps going on with diminishing values. When all the segment values have been determined up to a suitable total delay, the intensity at any point in the room may be determined by simple summation over Tx and all the wall segments (solid lines in Fig. 1). The numerical process is fast since it is only simple forward stepping in time.

The coupling between the segments is given by a square symmetric matrix $\mathbf{S}$ with elements

$$S_{ik} = \frac{\rho}{\pi} \cos\theta_i \cos\theta_k \frac{1}{R_{ik}^2} \Delta S \tag{1}$$

where ρ is the power scattering (reflection) coefficient ($0 \leq \rho \leq 1$), θ_i and θ_k are the angles from the normals of the respective segments i and k, and R_{ik} is the distance between segment centers. The size of the segments ΔS should be small enough to represent the geometry of the room with reasonable accuracy, but too small size would result in a high number of segments and correspondingly in high memory demands and running time. The time stepping algorithm for power of i-th element in time t, $P(t,i)$, is then

$$P(t,i) = P_{\mathrm{d}}(t,i) + \sum_{k=1}^{M} P(t-\tau_{ik},k) S_{ik}, \tag{2}$$
$$t = n\Delta t, n = \{1,\ldots,N\},\ i = \{1,\ldots,M\},$$

where all delays are rounded to the nearest multiple of Δt (the time resolution). The algorithm is running for N time steps, basically until all the powers drop below certain agreed level, which can represent the noise floor. The summation is over all M segments in the room—it encompasses segments on all reflecting walls and obstacles. The delay τ_{ik} is the delay between segments i and k. The summation over k is performed for each value of t and i, ensuring that all the multiple interactions are taken into account. P_{d} is the power of the direct signal from Tx, which is non-zero only at time instant τ_i corresponding to time delay between Tx and the segment i with distance R_i, assuming a gain of 1

$$P_{\mathrm{d}}(\tau_i,i) = \cos\theta_i \frac{1}{4\pi R_i^2} \Delta S, \tag{3}$$
$$i = \{1,\ldots,M\}.$$

The field at an arbitrary point inside the room is determined analogously to the update scheme (2), where the receiver stands for additional scattering segment (without re-scattering though) having the incident directivity constant over all angles, $\cos\theta = 1$, and equivalent surface of $\lambda^2/4\pi$ with λ being the wavelength at the center frequency of the pulse. Note that this

is the only place where frequency appears in the theory, and it only influences the levels of the received power, not the shape of the response. Also, a real antenna directivity could be added, if wanted.

To avoid any energy losses, the following inequality must be satisfied

$$\min R \geq \frac{c\,\Delta t}{2}, \tag{4}$$

that is, the shortest distance between any two segments must be at least as long as half the distance which the wave travels in one time step. This condition serves to ensure that all delays between segments will be nonzero after rounding to integer number of time steps. Zero delay would give rise to infinite values of power at the affected segments, or would have to be neglected otherwise, leading to nonphysical dissipation.

One theoretical limitation of the model is the extent of roughness of the walls. A room with perfectly smooth walls will not be characterized satisfactorily, in such a case ray tracing should be used instead. Also, the scattering cross sections of the walls are not known exactly and we use simplified assumptions of uniform diffuse scattering and absorption coefficient. Last but not least, polarization effects are entirely neglected in the present version of the algorithm.

III. Numerical Example

In the following, a numerical simulation of a rectangular room at frequency 5.9 GHz is performed, with receiver locations chosen in various distances from the transmitter. The room dimensions are width 11 m, length 19 m and height 2.5 m. Segment size has been chosen 0.5 × 0.5 m and the timestep Δt is 2 ns, obeying (4) in the corners. Transmitter location is at (x_{Tx},y_{Tx}) = (2,6) near the left wall and receiver locations are (x_{Rx},y_{Rx}) = (4,6), (8,6), (12,6), (16,6). In all instances, the z (vertical, height) coordinates are 1.5 m. The coordinate origin (x,y,z) = (0,0,0) is at the lower left corner. Both the transmitter and the receivers are omnidirectional in our simulations, although adding the respective radiation patterns into the computation is straightforward. The scattering coefficient ρ is 0.5. Fig. 2 shows the responses at the receiver locations and Fig. 3 shows $P(t,i)$ along the circumference of the room at the height of 1.25 m.[1] All power levels are expressed in dBW with unit reference (1 W Tx output power).

The first 60 ns are dominated by the incident fields—all of the curves in Fig. 2 show similar behavior in that there is a gap between the direct path (the first arrival) and the diffuse power reflected from the walls. However, the gap is not so deep at the receivers farthest away, indicating the influence of the floor and ceiling scatter. After that, the power falls off approximately exponentially with approximately the same power level at all receiver locations and also along the complete circumference (Fig. 3). This is in agreement with the theory and the experimental results. The decay rate is about 19 dB/100 ns. The slope could be changed by choosing another effective value of ρ. The simulation involved a total of 2272 wall segments and took approximately 2 min. on an average computer with Pentium 4 at 2.8 GHz.

[1]This height corresponds to the centers of the 0.5 × 0.5 m panels, into which the walls are discretized, at approximately the same height as the transmitter. To obtain the responses at the exact height of the transmitter would need some kind of interpolation, which we wanted to avoid for simplicity.

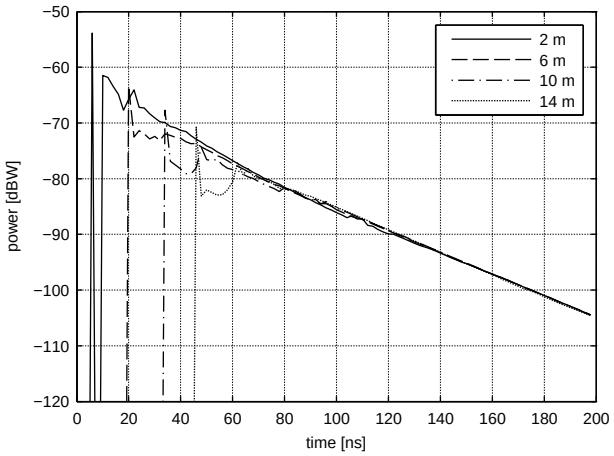

Fig. 2. Impulse responses at different distances from the transmitter.

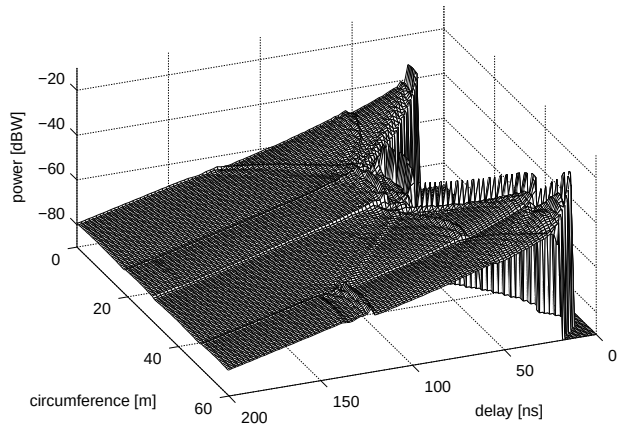

Fig. 3. Impulse responses along the circumference of the room at height 1.25 m.

For comparison, in Fig. 4 we also show the power delay profiles at various positions around the room obtained by measurement published in [4]. The room has the same dimensions as in the present numerical model, although it has windows and several obstacles scattered around it. The power distribution at all probe positions is again practically uniform after 60 ns and follows similar decay rate of 18 dB/100 ns. The absolute power levels are not directly comparable, as the calibration for the measurement was slightly different, namely the time integration window was larger resulting in higher magnitudes of power.

1) Power distributions and Rice factor: Since the direct line-of-sight (LOS) path is available as well as the diffuse part, it is possible to calculate the Rice factor, which is the ratio of the coherent and the integrated incoherent power. The LOS power is given as the peak value of the power delay profile

$$P_{\mathrm{LOS}} = \max P(t) = P(t_{\max}) \tag{5}$$

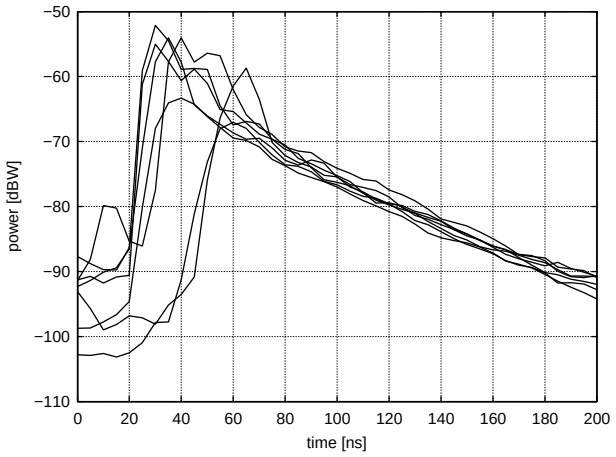

Fig. 4. Impulse responses at various positions around the room obtained by measurement [4].

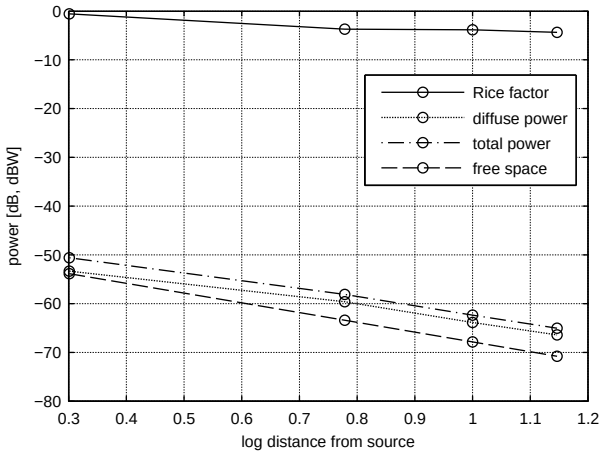

Fig. 5. Rice factor (7) in dB, the diffuse power (6), the total power (8), and the LOS power (5) versus log of distance in meters.

occuring at time instant $t_{\max}$ and the diffuse part is calculated as a sum of all values following $t_{\max}$

$$P_{\text{diff}} = \sum_{\tau=t_{\max}+1}^{N} P(\tau). \tag{6}$$

The Rice factor K is then their ratio

$$K = \frac{P_{\text{LOS}}}{P_{\text{diff}}}, \tag{7}$$

whereas the total power is their sum

$$P_{\text{tot}} = P_{\text{LOS}} + P_{\text{diff}}. \tag{8}$$

These indicators are shown in Fig. 5 in dB scale. The Rice factor is approximately leveled for the three outermost receivers, whereas the LOS and the tail decay at the same rate, which is a direct outcome of the presence of vertical scattering. However, between the first and the second receivers, the Rice factor is a decaying function of distance because the diffuse power (lower curve) decreases more slowly than the LOS power. Overall, the Rice factor is very small, indicating that the propagation channel follows rather Rayleigh fading, or, expressed differently, the distance is larger than the reverberation distance.

2) Angular response: For MIMO (multiple-input and multiple-output) applications the angular response is relevant, and this is easily found since all the scattering strengths and corresponding angles from the receiver are known from (2), see Fig. 6. It is noted that the angular spreading is almost uniform after about 100 ns. Before that the response is dominated by the single scattering.

3) Mean power: Finally, Fig. 7 shows the distribution of the mean power, i. e. the power integrated over the whole impulse response, across the room at height 1.5 m from the ground (the same height as the transmitter). As expected, the power decreases monotonically with distance from the transmitter, although there is apparent sign of leveling at the opposite wall, caused probably by multiple reflections. However, this view illustrates the potential of the algorithm for coverage predictions.

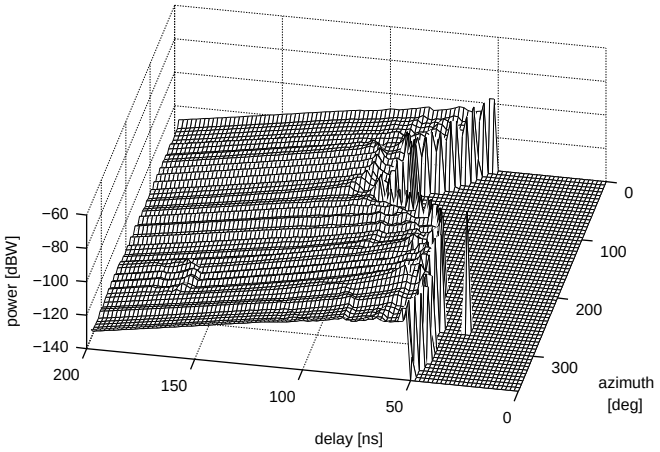

Fig. 6. Angular response at one position (12,6) from access point at (2,6).

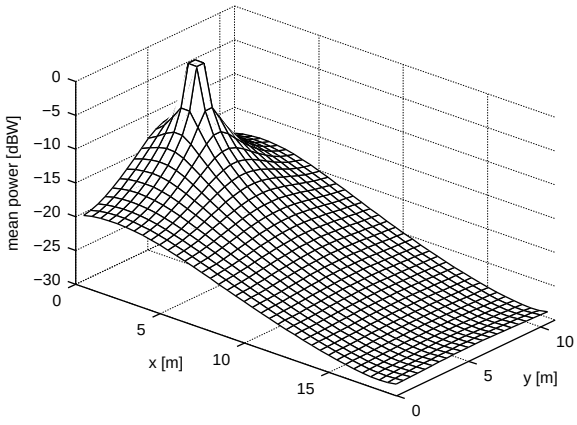

Fig. 7. Mean power distribution across the room at height 1.5 m from the ground.

The discretization of the walls into 0.5 m segments has been chosen in order to achieve sufficient accuracy of the algorithm while keeping the computational burden low. If we choose double resolution, i.e. 0.25 m, the segments will be $4\times$ smaller and the total number of segments M $4\times$ larger. Hence, the scattering matrix $\mathbf{S}$ (1) will have $16\times$ more elements with corresponding memory demands. Moreover, the update sequence (2) will be expected to take $32\times$ more time as a result of the increased number of elements and the necessity to halve the time step as well due to (4). These projections of the running time are of course purely theoretical and the actual timing might differ, nevertheless it gives the programmer an important idea about the scaling of the algorithm.

Apart from the presented algorithm, we also tried a simplified 2.5-dimensional version where only the circumference walls were taken into account and floor and ceiling virtually did not exist. The 2.5D version had even smaller computational demands, but the physical interpretation of the results was problematic, despite quite remarkable qualitative similarities to full 3D. We therefore concluded that the 3D algorithm is preferable, it is resonably fast and this would only improve with computer developments.

IV. Discussion

As can be seen in Fig. 2, as well as in experimentally obtained Fig. 4, the slopes of the response curves are everywhere the same inside the room. They are related to reverberation time T known from acoustics theory:

$$W = W_0 \mathrm{e}^{-\frac{t}{T}} \tag{9}$$

Here, W stands for energy in the room with initial value W_0, and t is the time variable. The reverberation time can be obtained from

$$T = \frac{4V}{c\eta A}, \tag{10}$$

which is commonly referred to as Sabine's law [11]. V and A are the volume and total surface area of the room, respectively, c is the velocity of light and η is the absorption coefficient of the walls, $\eta = 1 - \rho$. Generally, Eq. (10) is only an approximation for small η; larger values can be accommodated by Eyring formula, which results from (10) when η is substituted by

$$\eta' = -\log(1-\eta). \tag{11}$$

Formulas (10) and (11) assume equal probability for all ray paths, which is not generally true for rectangular rooms. Kuttruff proposes further correction by

$$\eta'' = \eta' \left(1 - \frac{\gamma^2}{2}\eta'\right), \tag{12}$$

where γ^2 is a parameter that accounts for the shape of the room. It can be obtained from numerical calculations and its values vary between 0.3–0.6 for rectangular rooms [11].

Our room has $\eta = 0.5$ and the slope of the decay curve in Fig. 2 is 19.4 dB/100 ns. The closest to this result is Kuttruff's correction by (12) giving 20.2 dB, while Eyring formula (11) gives 24.5 dB and Sabine's law alone (10) 17.7 dB. The γ^2 parameter was taken 0.51 after [11], where this value has been obtained by Monte Carlo method for room with relative dimensions 1:5:10, similar to our room.

Fig. 8 shows the power at three walls of the room (the other three are symmetric) after 300 ns from the initial pulse launch. The contour values are in dB with respect to the reference at the center of the floor, where the power level dropped to -108.8 dBW. It can be seen that even after a long time from the initial excitation the power distribution around the room is not entirely homogeneous, although it gradually drops with the same decay rate, in this case 19.4 dB/100 ns. In fact, in this simulation, the relative power distribution remained unchanged after capturing the field in Fig. 8, only the overall level was decreasing. We can see that the power at the walls is stronger on the longer ends of the room, whereas the floor and the ceiling have the lowest levels, and the power distribution has its maximum in the centers of the walls and is diminishing towards the corners. From here it follows that (10) and (11) can indeed be only approximative, since they rely on homogeneity of the field across the room.

It should be noted that Fig. 8 also shows one unphysical artifact, namely that the power levels are elevated in the corners of the room. This effect comes from the approximative nature of (1), in which coupling is strongly overestimated for segments very close to each other.

For comparison, an exact solution of the reverberation time is available for a sphere of diameter D, given by [12], [13]:

$$\eta = 1 - \frac{1}{2}\mu\left[\mu^{-1} + \mathrm{e}^{\mu}\left(1-\mu^{-1}\right)\right]^{-1}, \tag{13}$$

where $\mu = D/cT$. Although this formula was derived for the sound waves, it is as well applicable to electromagnetic wave propagation provided that it obeys Lambertian diffuse scattering and polarization effects are neglected, which is the case that is studied in the present paper. The reverberation time is obtained by solving (13) implicitly and gives 6.5 dB/100 ns.

Numerical calculation was carried out for sphere of diameter 20 m, see Fig. 9. The source is positioned in the center of the sphere, and the responses are taken by omnidirectional probes at distances 2, 4, 6 and 8 m from the center. The time step is again 2 ns and the mesh size is at least 0.5 m, and smaller towards the poles as it follows spherical coordinates. The frequency was again 5.9 GHz, but it is in fact irrelevant, because in this example we are interested in the decay rate only. The slope of the decay is 6.4 dB/100 ns, which we consider as a very good match and a proof of validity of the algorithm.

The calculations presented in this section are carried out for rooms with constant reflection (and, correspondingly, absorption) coefficient along the walls, which was also the case of the numerical examples. Realistic rooms will, of course, have different coefficients for various materials in the room (carpets, bookshelves, windows) and the responses will show irregularities, but the overall trends in decay will be similar. The conclusions should therefore be understood rather qualitatively, or in the sense of rooms with all coefficients averaged.

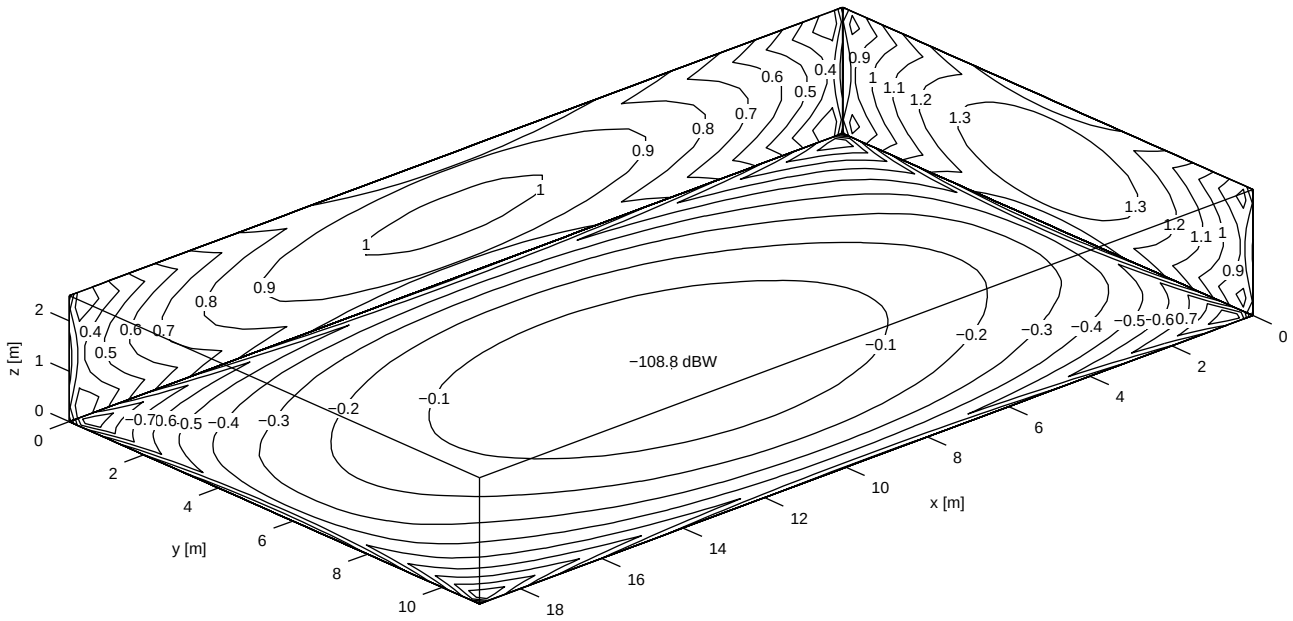

Fig. 8. Relative distribution of power in dB on the walls of the 19×11×2.5 m room after 300 ns.

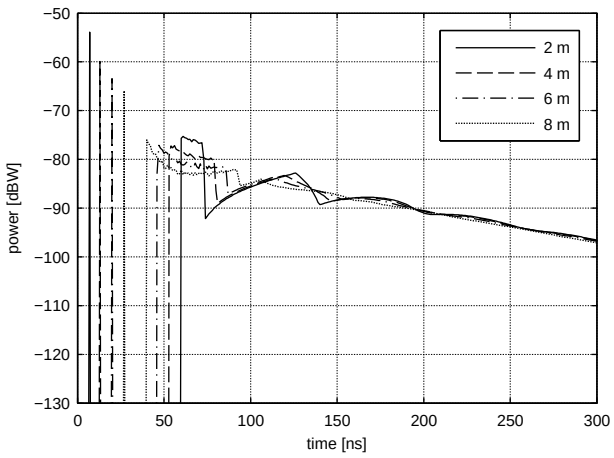

Fig. 9. Impulse responses at different distances from the transmitter at the center of the sphere with diameter 20 m.

V. Conclusion

It has been shown that the radiosity method is capable of predicting electromagnetic reverberation times which fit well with theory, the difference between the simulation and Kuttruff's corrected reverberation formula is only 0.8 dB/100 ns. The presented room responses are also noted to be in agreement with previous measurements in an office space of similar dimensions [4], although the equivalent value of the absorption coefficient (0.5) for the practical case is debatable. Validity of the algorithm has been verified by comparing the results to exact solution for a spherical cavity, where excellent match within 0.1 dB has been obtained. However, we conclude that the theoretical values for reverberation given by Sabine and Eyring are only informative when it comes to rectangular rooms and, by generalization, rooms of arbitrary shape. Limited accuracy of the theoretical formulas thus highlights the importance of the presented algorithm for general, complicated shapes of rooms.

Even though the numerical experiment involved an empty rectangular room only, the algorithm can be easily applied to more complex indoor and also outdoor scenarios, and the computational burden is not expected to be tremendous. Only 2272 wall segments with 0.5 × 0.5 m size were used, being quite large with respect to the wavelength of 5 cm at frequency 5.9 GHz, and still achieving very good accuracy. This is a clear advantage to other methods (FDTD for example) which rely on sufficient spatial discretization of the waves and usually need many samples per wavelength.

The numerical algorithm is also general enough to accommodate objects of arbitrary shape in the room (people, furniture), which will be represented by additional scattering segments. Nevertheless, the presence of such obstacles is already included in the diffuse characteristics of the walls and, therefore, adding them into the simulation as separate objects might not yield substantially different result. The numerical model is indeed very simple, yet it agrees very well with theory and experimental results, and, therefore, provides useful prediction of radiowave coverage in rooms.

Acknowledgment

The authors would like to thank the TAP reviewers and Dr. Tim Brown for their useful comments on the manuscript.

References

[1] R. Valenzuela, "A ray tracing approach to predicting indoor wireless transmission," in *1993 IEEE 43rd Vehicular Technology Conference*, May 1993, pp. 214–218.

[2] R. Vaughan and J. B. Andersen, *Channels, Propagation and Antennas for Mobile Communications*. London: IEE, 2003.

[3] A. Valcarce, G. De La Roche, Á. Jüttner, D. López-Pérez, and J. Zhang, "Applying FDTD to the coverage prediction of WiMAX femtocells," *EURASIP Journal on Wireless Communications and Networking*, vol. 2009, pp. 1–13, 2009.
[4] J. B. Andersen, J. Ø. Nielsen, G. F. Pedersen, G. Bauch, and M. Herdin, "Room electromagnetics," *IEEE Antennas Propag. Mag.*, vol. 49, no. 2, pp. 27–33, Apr. 2007.
[5] E.-M. Nosal, M. Hodgson, and I. Ashdown, "Improved algorithms and methods for room sound-field prediction by acoustical radiosity in arbitrary polyhedral rooms," *The Journal of the Acoustical Society of America*, vol. 116, no. 2, pp. 970–980, 2004. [Online]. Available: http://link.aip.org/link/?JAS/116/970/1
[6] I. Ashdown, *Radiosity: A Programmer's Perspective*. New York: Wiley, 1994.
[7] C. Kloch and J. B. Andersen, "Radiosity—an approach to determine the effect of rough surface scattering in mobile scenarios," in *IEEE Antennas and Propagation Society International Symposium 1997 Digest*, vol. 2, Jul. 1997, pp. 890–893.
[8] C. Kloch, G. Liang, J. B. Andersen, G. F. Pedersen, and H. L. Bertoni, "Comparison of measured and predicted time dispersion and direction of arrival for multipath in a small cell environment," *IEEE Trans. Antennas Propag.*, vol. 49, no. 9, pp. 1254–1263, Sep. 2002.
[9] M. Liang and Q. Liu, "A practical radiosity method for predicting transmission loss in urban environments," *EURASIP Journal on Wireless Communications and Networking*, vol. 2004, no. 2, pp. 357–364, 2004.
[10] G. Rougeron, F. Gaudaire, Y. Gabillet, and K. Bouatouch, "Simulation of the indoor propagation of a 60GHz electromagnetic wave with a time-dependent radiosity algorithm," *Computers & Graphics*, vol. 26, no. 1, pp. 125–141, 2002.
[11] H. Kuttruff, *Room acoustics*, 4th ed. London: Taylor & Francis, 2000.
[12] M. M. Carroll and C. F. Chien, "Decay of reverberant sound in a spherical enclosure," *The Journal of the Acoustical Society of America*, vol. 62, no. 6, pp. 1442–1446, 1977. [Online]. Available: http://link.aip.org/link/?JAS/62/1442/1
[13] W. B. Joyce, "Exact effect of surface roughness on the reverberation time of a uniformly absorbing spherical enclosure," *The Journal of the Acoustical Society of America*, vol. 64, no. 5, pp. 1429–1436, 1978. [Online]. Available: http://link.aip.org/link/?JAS/64/1429/1

Ondřej Franek (S'02–M'05) was born in 1977. He received the M.Sc. (Ing., with honors) and Ph.D. degrees in electronics and communication from Brno University of Technology, Czech Republic, in 2001 and 2006, respectively. Currently, he is working at the Department of Electronic Systems, Aalborg University, Denmark, as a postdoctoral research associate. His research interests include computational electromagnetics with focus on fast and efficient numerical methods, especially the finite-difference time-domain method. He is also involved in research on biological effects of non-ionizing electromagnetic radiation, indoor radiowave propagation, and electromagnetic compatibility.

Dr. Franek was the recipient of the Seventh Annual SIEMENS Award for outstanding scientific publication.

Jørgen Bach Andersen (LF'92) received the M.Sc. and Dr.Techn. degrees from the Technical University of Denmark (DTU), Lyngby, Denmark, in 1961 and 1971, respectively. In 2003 he was awarded an honorary degree from Lund University, Sweden. From 1961 to 1973, he was with the Electromagnetics Institute, DTU and since 1973 he has been with Aalborg University, Aalborg, Denmark, where he is now a Professor Emeritus and Consultant. He was head of a research center, Center for Personal Communications, CPK, from 1993–2003.

He has been a Visiting Professor in Tucson, Arizona, Christchurch, New Zealand, Vienna, Austria, and Lund, Sweden. He has published widely on antennas, radio wave propagation, and communications, and has also worked on biological effects of electromagnetic systems. He has coauthored a book, *Channels, Propagation and Antennas for Mobile Communications*, IEE, 2003 with Rodney G. Vaughan. He was on the management committee for COST 231 and 259, a collaborative European program on mobile communications. He is Associate Editor of 'Antennas and Wireless Propagation Letters', and Co-Editor of a forthcoming joint special issue of IEEE Transactions on Antennas and Propagation and Microwave Theory and Techniques on 'Multiple-Input Multiple-Output (MIMO) Technology'.

Professor Andersen is a former Vice President of the International Union of Radio Science (URSI) from which he was awarded the John Howard Dellinger Gold Medal in 2005.

Gert Frølund Pedersen was born in 1965, is married to Henriette and has 7 children. He received the B.Sc.E.E. degree, with honour, in electrical engineering from College of Technology in Dublin, Ireland, and the M.Sc.E.E. and Ph.D. degrees from Aalborg University in 1993 and 2003. He has been employed by Aalborg University since 1993 where he is now full Professor heading the Antennas, Propagation and Radio Networking group and is also the head of the doctoral school on wireless which has close to 100 Ph.D. students enrolled. His research has focused on radio communication for mobile terminals, and especially on small antennas, diversity systems, propagation and biological effects, and he has published more than 75 peer reviewed papers and holds 20 patents. He has also worked as consultant for developments of more than 100 antennas for mobile terminals including the first internal antenna for mobile phones in 1994 with lowest SAR, first internal triple-band antenna in 1998 with low SAR and high TRP and TIS, and lately various multi antenna systems rated as the most efficient on the market.

He has been one of the pioneers in establishing the over-the-air measurement systems. The measurement technique is now well established for mobile terminals with single antennas and he is now chairing the COST2100 SWG2.2 group with liaison to 3GPP for over-the-air tests of MIMO terminals.